Desalination and Water Treatment
www.deswater.com

doi: 10.1080/19443994.2014.978390

57 (2016) 1634–1646
January

Taylor & Francis
Taylor & Francis Group

Synthesis of an electrically cleanable forward osmosis membrane

Zubin M. Darbari, Alka A. Mungray*

Department of Chemical Engineering, S. V. National Institute of Technology, Surat 395007, Gujarat, India, Tel. +91 261 2201716, +91 261 2201901; Fax: +91 261 2201605; emails: bag@ched.svnit.ac.in, boricha_alka@yahoo.co.in

Received 20 March 2014; Accepted 9 October 2014

ABSTRACT

A novel way to remove fouling from forward osmosis membrane is carried out in this research work. Electric field was used as a novel fouling removal option in this research work. Therefore, conductive membrane was prepared with the use of chitosan (CHS), polyvinyl alcohol (PVA), and graphene (Gr). The prepared membrane named as "CHS/PVA/Gr". Various characterization methods are used to characterized this CHS/PVA/Gr membrane i.e. conductivity, porosity, swelling ratio, water flux measurement, and scanning electron microscopy (before and after fouling). To check the CHS/PVA/Gr membrane performance and fouling behavior forward osmosis (FO) experiments are carried out with distilled water (DI water) and algae-containing water. In FO experiments, as a feed solution algae water (nearby lake water) and as a draw agent, high concentration NaCl solution (4 M NaCl) was used. Membrane fouling and draw solution leakage was investigated in this research work by laboratory-scale forward osmosis (FO) setup. The water flux in FO mode was 31.2 $Lm^{-2} h^{-1}$ (LMH) (with DI water as a feed) and reverse salt diffusion 0.015 $gm^{-2} h^{-1}$ (gMH). The initial FO water flux value is 28.1 LMH with algae-containing water. Intention of fouling removal method is to regain the initial water flux after giving cleaning treatment in IC current the form of elect. After cleaning experiments, the restore water flux values are 14.2 and 22.04 LMH for distilled water and electric field cleaning method, respectively.

Keywords: Forward osmosis; Membrane; Electric field; Fouling

---

1. Introduction

Water scarcity is a major problem for almost all countries of the world. This need can be satisfied by claiming water from various non-conventional sources such as wastewater and sludge. Water purification can be done by methods such as electrolysis, distillation, and membrane filtration. Among these, electrolysis is not practical as it consumes huge amount of energy. Distillation is not useful because of it is for fractions with high vapor pressure and boiling point near to water. Hence, membrane filtration is an effective way for production of water.

Forward osmosis (FO) and pressure-retarded osmosis (PRO) are emerging osmotically driven membrane processes, where water is driven through a semipermeable membrane from a feed solution (FS) of low osmotic pressure to a draw solution (DS) of high osmotic pressure. Forward osmosis does not require an applied pressure. Forward osmosis has potential applications including seawater and brackish water desalination.

---

*Corresponding author.

Forward osmosis (FO) process can serve as alternative process to RO to desalinate water at reduced cost as it operates at low or no pressure. Fouling is one of the main challenges in the FO process. Solute or particles in feed water deposit onto the membrane surface in such a way that causes flux decline, this process is known as fouling and it affects the quality and quantity of the water recovered. The decline of flux due to membrane fouling is a big problem in waste-water treatment as it significantly affects the performance. Studies have been carried out to find out various methods of reducing fouling, i.e. feed water pretreatment, increasing antifouling properties of membranes, and optimizing operating conditions [1–5]. In FO process, both sides of the FO membrane are in constant contact with impaired waters: the active layer with wastewater effluent and the support layer with seawater or brine. So, understanding the fouling behavior in the osmotic dilution process becomes particularly important. Due to this, a critical need arises for a systematic understanding of membrane fouling behavior and development of strategies for fouling mitigation [6]. Backwash of membrane with DI (distilled) water at different cross-flow velocity is one of the most popular and easy way to remove fouling in FO. Some papers are available on backwash and tabulated in Table 1. Different types of nanoparticle coating/incorporation on membrane were used by some researchers to remove fouling. In a recent study, antibacterial Ag nanoparticles are used in layer-by-layer manner in FO membrane for fouling removal [7]. The performance of fouled FO membranes can be partially restored by selecting appropriate cleaning methods. Cleaning methods generally require some cleaning agents, for example, strong alkali, acids, and surfactants. [8]. Table 2 gives clear-cut idea about the currently used common fouling control strategies. Control strategies' effectiveness appeared to be very site specific. Integrating approaches by coupling, adequate pretreatment with selection of the proper membrane module and operating conditions are essential to mitigate fouling problems efficiently and economically. Some research works are carried out on special type of membrane module process named as "vibratory shear enhanced process" (VSEP). VSEP is an alternative approach to the aforementioned dynamic filtration. The membrane module moves in a vigorous vibratory motion, tangent to the face of membranes, creating shear waves of fluid that prevent membrane fouling. VSEP filtration has been previously applied in certain cases, such as for the purification of pulp and mill paper re-circulation water [9], and treatment of yeast dispersions and bovine albumin solutions [10], treatment process of dairy waters [11]. Furthermore, as it was reported by Takata et al. (1998), the VSEP filtration module was effective for the prevention of fouling for treatment of river water. But due to high cost of this equipment, it cannot be widely accepted [12].

All fouling reducing options are costly and inevitably increase operation difficulty, decreasing membrane's life, which will be translated into higher costs. From VSEP, it is confirmed that vibrating action is an effective method for fouling removal. Therefore, researchers are trying to find out other options, which are highly effective and less costly.

Chitosan (CHS) which is the deacetylated form of biopolymer chitin. It is the second most abundantly available biopolymer in nature after cellulose. It is an extremely hydrophilic material. Presence of reactive amino and hydroxyl groups in the chitosan is responsible for the hydrophilicity [13]. But its use is restricted due to its unfavorable mechanical properties.

There is a need to find an alternative for fabrication of FO substrate, which can fulfill the FO requirements. Polyvinyl alcohol (PVA) is a synthetic polymer, which has high hydrophilicity and soluble in water that allow for better dispersion of any organic/inorganic filler. Furthermore, PVA films are flexible as well as possessing good dimensional stability [14]. PVA is a very popular polymer to fabricate pervaporation membrane for dehydration of organic solvents e.g. methanol [15]. For the forward osmosis membrane, supporting layer must be highly hydrophilic. But due to the hydrophobicity of PS and PES is not possible to use these polymers. Therefore, in our study highly hydrophilic PVA and chitosan were used [16,17].

Polymer composites, filled by graphitic nanostructures, due to their unique mechanical, electrical, and optical properties have attracted increased attention [18]. Nanosized conductive fillers, including graphene nanoplatelets, create a percolative network within the polymer matrix at a low weight fraction, graphene, a two-dimensional sheet of covalently bonded carbon atoms. It is one of the strongest materials (tensile strength 1TPa). It has high surface and size selective porosity. It has attracted interest as a material with potential use in various applications such as touch panels, p–n junction materials, flexible thin-film transistors, and solar cells. [19,20].

Graphene/PVA composite samples were prepared in the literature. Researchers observed enhanced thermal stability for their composites bearing graphene loading above 1 wt%, comparing to the pristine matrix (PVA) [21].

Graphene has zero band gap, which lead to its use in place of Si in electronics but on making transistors

Table 1
Cleaning of FO membranes with DI water

Membrane	Draw Solution	Feed Solution	Cross flow velocity	pH	Temp (°C)	Cleaning method	Percentage regeneration/cleaning	References
Membrane was provided by Hydration Technologies, Inc. (Albany, OR). It has an asymmetric structure and is made of cellulose acetate supported by embedded polyester mesh, having thickness ~50 μm	1.5 M–4 M NaCl	50 mM NaCl, some 0.5 mM $CaCl_2$, 200 mg/L foulant [(a) BSA (Mo.wt 66kDa), (b) sodium alginate from brown seaweed, (Mo.wt 12–80kDa), (c) AHA (10g/L)]	8.5 cm/s	(a) 6.3 (b) 5.8 (c) 6.2	20 ±1°C	20–24 h Fouling		[39]
FO membrane by HTI	1.5 M MgSO4·7H2O, NaCl, NaNO3 and ZnSO4·7H2O solutions in deionized (DI) water by Mili-Q plus device was used as draw solutions	Activated sludge fouling for 7–8 h	Flow rate 5.5 L/min		20 ± 2°C	DI water	Negligible fouling present	[40]
Cellulose Acetate Embedded by Polymer mesh (Hydration Technologies Inc) Thickness ~50 μm	4 M NaCl	200 mg/L alginate, 50 mMNaCl, and 0.5 mMCa2+	8.5 cm/s	5.8	20 ± 1°C	50 mM NaCl: (a) 1 hr, 8.5 cm/s (b) 5 hr, 8.5 cm/s (c) 24 hr, 8.5 cm/s (d) 15 min, 21 cm/s	(a) 64% (b) 86% (c) 96% (d) >98%	[41]
Cellulose triacetate (CTA) membrane from Hydration Technologies, Inc (Albany, OR)	4 M NaCl	NaCl 20 mM Alginate 200 mg/L Na_2SO_4 20 mM $CaCl_2$ 35 mM $NaHCO_3$ 1 mM	8.5 cm/s, 48 h	7.5		DI rinsing, Cross-flow: 21cm/s, 20 min	80%	[42]
Flat-sheet cellulose triacetate (CTA) FO membranes (Hydration Technologies, Albany, OR) water contact angles of selective (or active) layer and back (support) layer were (61.3° ± 0.8°) and (66.4° ± 1.3°)	1.5 M Na_2SO_4 (π_{draw} = 20 atm)	Brackish water equivalent to 0.06 M NaCl (π_{feed} = 10 atm)	25.0 cm/s	7.9	(a) 25°C (b) 35°C (c) 45°C	DI water at cross-flow of 33.3 cm/s for 20 min	J_i (a) 15.13, (b) 19.79, (c) 22.09 J_r (a) 15.08, (b) 16.80, (c) 17.50 (a) 99.7%, (b) 84.9%, (c) 79.2%	[43]

The FO membrane is made of cellulose triacetate (CTA) embedded in a polyester mesh support, with a thickness of 30–50 µm provided by Hydration Technology Innovations (HTI, Albany, OR, USA). (S = 595 µm)	DS, pre-filtered (0.45 µm pore size) Red Sea water was used as filtered seawater (FSW), seawater was obtained from the seawater pipeline of the RO plant operating at KAUST, TDS 40.5 g/L, DOC 1.12 mg/L, pH 7.8	Secondary wastewater effluent BOD 20 mg/L COD 20 mg/L Total Organic Carbon (TOC) 4.60 mg/L TSS 2.4 mg/L VSS 2.1 mg/L (from Al-Ruwais wastewater treatment plant in the city of Jeddah, Saudi Arabia)	0.06 cm/s	7.3	20 ± 0.5˚C	(a) air scouring for 15 min,at a cross flow rate of 4166 ml/min in the feed water tank, i.e. 3.13 L of air /L of feed water (for NOM) (b) 0.8% Na_2EDTA, 1% Alconox, a detergent composed of NaDBS (10–30%), Na_2CO_3 (7–13%), TSPP (10–30%) and sodium phosphate (10–30%), pH 8.0 (for TEP(+1% NaOCl) & SWWE)	(a) After day 13 90.8% (b) After day 14 88.9%	[25]
commercially available cellulose triacetate (CA) membranefrom Hydration Technology Innovations (Albany, OR)	4 M NaCl	Sodium alginate (75–100 kDa) 200 mg/L and gypsum (CaSO4·2H2O), added into 3.5 M $CaCl_2$, 1 M Na_2SO_4, with saturation index 1.3. for 48 h	8.5 cm/s	7.5	20 ± 1˚C	rinsing the membrane with DI water for 20 min at a cross-flow rate of 21 cm/s in the absence of permeate flux; air bubbles were continuously introduced to enhance cleaning	(a) Alignate(35 mM Ca^{2+}) ~ 10.2% (b) Gypsum + Alignate ~ 82% (c) Gypsum on Alignate ~62%	[44]
cellulose triacetate supported by embedded polyester mesh (by HTI)	0.5 M NaCl	Oil 0, 30, 300, 3000 mg/L and 30 mg/L NaCl	9 cm/s	7.38	25 ± 2˚C	Mili-Q water for 1 hr	91% (~10% decrease in flux after fouling)	[45]
Membrane made of cellulose triacetate is designated as CA membrane, which is manufactured by Hydration Technology Innovations (Albany, OR)	1.5–4 M NaCl (for 1 h, then cleaned) [repeat 24–72 h]	4.2 mM silica, 115 mM NaCl, and 19 mM $MgCl_2$, with a saturation index for amorphous silica of 2.2.	8.5 cm/s	6.2	20 ± 1˚C	DI water was used to rinse the Membrane for 15 min, crossflow velocity 21 cm/s	(a) 98% in silica scaling mode (4 M) (b) 80% in RO mode (c) ~99% in FO (1.5 M)	[46]

Table 2
Common strategies for controlling membrane fouling

Method references	
Direct methods	
Periodic hydraulic or chemical cleaning	[47]
Impulse feed	[48]
Turbulence promotor	[49]
Dean vortex	[50]
Rotating–vibrating membrane	[51]
Outside aeration	[52]
Inside gas sparging	[53]
Indirect methods	
Pretreatment by coagulation–filtration	[54]
Pretreatment by air flotation PAC addition	[55]
PAC addition	[56]
Membrane surface modification	[57]
Selecting optimum operating conditions	[58]
Changing operating modes	[59]

out of it, another of its unique properties was found out; it vibrates on applying A.C. voltage across it, i.e. reverse piezoelectric effect [22,23]. Its frequency is proportional to frequency of A.C. source and amplitude proportional to current. This also gave rise to nanoelectromechanical systems [24].

In this research work, we tried to use semiconductor industry's concept. When graphene is used to make transistors, it vibrates when current passes through it. This revolutionary property of graphene is used to vibrate prepared forward osmosis membrane in the presence of applied electric field to remove fouling. Therefore, an attempt is made to remove fouling from prepared CHS/PVA/Gr membrane by use of electric field. Up to authors knowledge not a single study/paper is available on this aspect.

2. Materials and methods

2.1. Materials

Chitosan was in the powder form (M/S. Marine Chemicals, Cochin, Kerala, India) with mean molecular mass of 1.25×10^5 and degree of acetylation 85%. Polyvinyl alcohol (PVA) (85–89% hydrolyzed and the weight-average molecular weight: 2000–95,000) was used as the polymer material for the fabrication of membrane substrate purchased from Fisher Scientific India. Distilled water of pH 5.9 ± 0.2, and conductivity 1.0 μS/cm (Millipore, Elix, Bangalore, India) is used throughout. Glutaraldehyde (GA) solution 25% (Merck, India) was used as a crosslinking agent. All the other laboratory grade chemicals (sulfuric acid and acetone) used were procured from Merck, India. Graphene nanoplatelets (average thickness: 1–5 nm, surface area: 500 and 750 m^2/g, average particle diameters: >2 microns, appearance: black granules/powder, oxygen content: <2 wt%, carbon content: >98.0 wt%). Polyvinylpyrrolidone (PVP) (average molecular weight = 40,000) from Heavy Chemicals Ltd is used in this research work.

2.2. Membrane preparation

2.2.1. Chitosan membrane

Chitosan solution was prepared by dissolving 15 g CHS in 85 g (2 wt%) acetic acid. The solution was stirred at 1,000 rpm (REMI model-R 24, India) for 12 h to get the homogeneous polymer mixture. The resultant homogeneous mixture was transferred to an airtight conical flask and kept for 24 h in a refrigerator for the removal of entrapped air bubbles. Cast the homogeneous solution using an automatic film applicator (Sheen Instrument Ltd, Vacuum based, Model number: 1,133 N) at a speed of 50 mm s^{-1}. The initial thickness of the casted film was adjusted by a four-sided applicator and air dried the prepared membrane.

2.2.2. Chitosan/PVA membrane

PVA aqueous solution was prepared by dissolving 10% by wt PVA into water at 100°C. Chitosan (prepared solution) and PVA solutions were mixed in 2:1 proportions. The solution was stirred at 200 rpm (REMI model-R 24, India) for 24 h to get the homogeneous polymer mixture. The resultant homogeneous mixture is transferred to an airtight conical flask. It was then refrigerated to remove entrapped air bubbles overnight and then membrane was cast as per the procedure described in Section 2.2.1.

2.2.3. Chitosan/PVA/graphene membrane

Above prepared chitosan/PVA solution was added in 32 mg graphene + 1,600(32 * 50) mg PVP in 160 mL water (10 mg of PVP/ml of water) using bath sonication till 1 h [25]. For 24 h, 4 mg graphene stoke solution was stirred and cast using an automatic film applicator (Sheen Instrument Ltd., Vacuum based, Model number: 1133 N) at a speed of 50 mm s^{-1}after the removal of bubbles. To increase conductivity, 4 mg graphene was also coated onto the prepared membrane, followed by dried at room temperature and then in vacuum oven at 50°C overnight to completely remove solvent for 1 h. The cured membrane was covered by the aqueous GA solution (0.25 wt%) and the excess solution is drained by holding the membrane vertically, followed by crosslinking at 40°C for 1 h. After crosslinking, the membrane was washed with deionized water extensively and immersed in deionized water for 5–6 h to remove the remaining unreacted glutaraldehyde. Before the FO experiment tests, the coated membrane was kept in water for some time to prevent crystal formation. Prepared three membranes named as "CHS", "CHS/PVA," and "CHS/PVA/Gr."

2.3. Characterization of membranes

2.3.1. Conductivity measurement

Conductivity of all three membranes was measured by conductivity meter (Mettler Toledo Greifensee, Switzerland).

2.3.2. Degree of swelling

Prepared membranes were immersed into deionized water at a desired temperature for 24 h to make the membranes saturated. Then the membranes were taken out, wiped with a tissue paper, and quickly weighted on a microbalance. Swelling ratio (SR) was calculated by the changes in weight between the dry and the fully hydrated samples as below Eq. (1).

$$\text{Swelling ratio }(\%) = \frac{(W_s - W_d)}{W_d} \times 100 \tag{1}$$

where W_d is the weight of the dry membrane and Ws is the weight of the membrane swollen in the solution.

2.3.3. Membrane porosity

To measure the porosity of CHS, CHS/PVA, and CHS/PVA/Gr membrane, dry membranes were weighted (m_{dry}) and same membranes were immersed in water for 1 h and blotted using tissue paper to remove the excess water on the surface. The wet membranes were then weighted (m_{wet}). Then, porosity ε (%) of the membranes was calculated using below Eq. (2) [26].

$$\varepsilon = \frac{(m_{\text{wet}} - m_{\text{dry}})/\rho_w}{[m_{\text{wet}} - m_{\text{dry}}/\rho_w] + m_{\text{dry}}/\rho_m} \times 100 \tag{2}$$

where ρ_w and ρ_m are the density of the wetting solvent (water in the current study) and membrane, respectively.

2.3.4. Macroscopic view of the membrane

Macroscopic view of the clean FO membrane and foul FO membrane was carried out by typical optical microscopic (Images ZMD, microscope p800).

2.4. FO performance evaluation of CHS/PVA/Gr membrane

The FO performance of the prepared membrane was evaluated using two equal-size compartments FO setup shown in Fig. 1. The total liquid volume of each compartment was 1.5 liters. The effective surface area of the membrane was 19 cm^2. The temperature of the feed and draw solution was maintained at room temperature of about 28 ± 2°C. During osmosis experiments, the draw and feed solutions were stirred using stirrer and the absence of feed spacer. CHS/PVA/Gr membrane performance was evaluated under FO (where the active-layer-facing feed solution (AL-FS)) mode. FO performance used an algae mixture (nearby lake view garden's lake water, Piplod, Surat) as the feed and 4 M NaCl as a draw solution. Algae mixture parameters are tabulated in Table 3. The prepared membrane CHS/PVA/Gr was stabilized until achieving the stable water flux i.e. at least 30 min. Then, the pure water flux was recorded as the average value of 10 min.

The water permeation flux from feed solution to draw solution was calculated from the volume change of the feed water by observing level change on feed compartment. The water flux (J_w, Lm^{-2} h^{-1}, abbreviated as LMH) is calculated from the volume change of the feed the solution using below Eq. (3).

$$Jw = \frac{\Delta V}{\Delta t A_m} \tag{3}$$

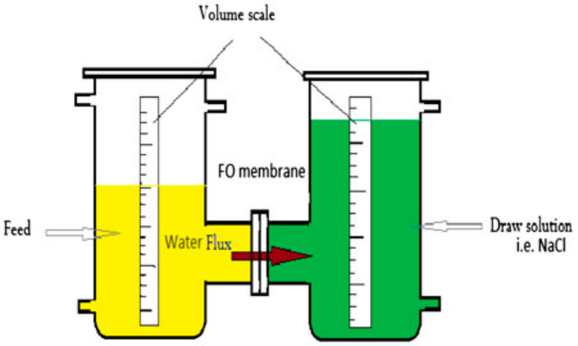

Fig. 1. Experimental setup for forward osmosis.
Notes: The following testing conditions were adopted for FO evaluation. Draw Solution (DS): 4 M NaCl concentration. Feed Solution (FS): Nearby lake algae containing water.

Table 3
Algae-containing water parameters

Parameters	Concentration (mg/L)
pH	8
TS	183.4
BOD_5	4.6
COD	8.7
DO	5.9
TDS	180.3

where ΔV is the volume change of feed solution, Δt is the measuring time interval, and A_m is an effective membrane area.

The salt concentration in the feed water solution was determined from the conductivity measurement based on the standard concentration-conductivity curve for NaCl. The reverse salt diffusion Js in $gm^{-2}\,h^{-1}$ (abbreviated as gMH) from the draw solution to the feed side was determined from the increase of the feed conductivity using below Eq. (4).

$$Js = \frac{\Delta(C_t V_t)}{\Delta t A_m} \tag{4}$$

where, C_t and V_t are the salt concentration and volume at the end of FO tests, respectively [27].

2.5. Organic fouling and cleaning experiments

2.5.1. Synthetic wastewater

The synthetic wastewater consists of (per L of DI water): glucose, 1,000 ± 10 mg; protein, 80 ± 5 mg; $NaHCO_3$, 24 ± 5 mg; KH_2PO_4, 14 ± 5 mg; NH_4Cl, 60 ± 5 mg; $CaCl_2$, 18 ± 3 mg; and $MgSO_4{\cdot}7H_2O$, 24 ± 3 mg [28]. The pH of synthetic wastewater was 7.32 in anode, and the pH was adjusted by 0.1 M potassium phosphate buffer solution. Parameters of synthetic wastewater are shown in Table 4. Synthetic wastewater was taken in a petri dish and prepared CHS/PVA/Gr membrane was dipped in for 45 min, and then dried. As the membrane was a bit degraded as chitosan is biodegradable, as well as some of the graphene fell off as it was physically plated and could not be done chemically as it will change its resonating properties. A. C. voltage was applied to membrane to remove fouling but not as much as expected due to loss of graphene.

Table 4
Parameters of synthetic wastewater

Parameters	Concentration
Conductivity	5,841 μs/cm
pH	6.12
ORP	29 mV
DO	5.02 mg/L
COD	1,086 mg/L

2.5.2. Algae-containing water

For the baseline experiments, the feed solution was prepared using NaCl in the absence of organics (i.e. no stock solution was used in the feed). Constant molar feed and draw solution concentrations were maintained throughout the duration of each experimental run. The procedure was given as below, at every ten-minute interval, the conductivity of the feed and draw solutions was measured using conductivity meter and the corresponding molarity of the solutions was deduced from a calibration curve. Subsequently, requisite proportion of NaCl was added to make the concentration of the draw solution constant at 4 M. Similarly, appropriate volume of DI water was added to the feed solution side to maintain a constant feed ionic strength. Thus, the water flux was representative of the inherent membrane fouling over the experimental duration. For FO experiments, the CHS/PVA/Gr membrane was first stabilized for at least 30 min, with deionized water as a feed and 4 M NaCl as the draw solution, until achieving the stable water flux. Then, the pure water flux was recorded as the average value of 10 min. The next stage, in which an algae (lake view garden's lake water, Piplod, Surat) containing solution was used as the feed solution instead of DI water and 4 M NaCl as the draw solution. Water flux was again checked in FO mode at equal time interval for eight hrs. After that, two ways are used to remove fouling for comparison purpose. First, in the DI water cleaning process, both the feed and draw solutions were changed into deionized water to rinse the membrane. After one hour rinsing, the pure water flux of the membrane was measured according to Eq. (3) with deionised water as the feed solution and 4 M NaCl as the draw solution. The pure water flux was calculated again after cleaning to examine the removal of the fouling from the FO membrane. In second way, an electric field was applied for the cleaning process (see Fig. 5). The foul membrane was cleaned approximately 1 h by giving A.C. voltage without disturbing the process. When electric field was applied, the voltage was supplied from a steady DC power source.

Eq. (5) given below is used for the determination of flux recovery by both the cleaning process [27].

$$\% \text{ Flux recovery} = \frac{J_f}{J_i} \times 100\% \tag{5}$$

where J_i is the average flux recorded for the initial or referential cycle and J_f is the average flux recorded for a cycle run after a certain cleaning technique was used.

3. Results and discussion

3.1. Conductivity measurement

Measured conductivity values are tabulated in Table 5. Table 5 clearly indicate that the addition/coating of graphene in membrane increase the conductivity value. In the literature, one research study is based on graphene/poly(vinyl chloride) composite thin films. They have concluded that the conductivity increases drastically up to 0.6 vol.% of graphene, above which the rate of increase was minimum [28]. In the literature, many papers are concluded that graphene addition in polymer matrix increases conductivity i.e. graphene and poly (3,4-ethyldioxythiophene) [29], polyaniline/graphite [30]. The graphene CHS/PVA/Gr modified membrane had better conductivity than that of CHS and CHS/PVA membrane. Incorporation and coating of Gr in membrane improved the conductivity of the membranes [31]. It is obvious that the addition of graphene into the polymer matrix has a significant influence on its mechanical behavior. Almost all the polymer/graphene composites reported in the literature described the electrical conductivity of the composites, which varies widely and generally increases with increasing graphene loading [32]. For example, the introduction of graphene (1.4 wt%) results in a maximum increases of 72.9% in the tensile strength for the dry states [33].

3.2. Degree of swelling

In our study, swelling ratio of CHS and CHS/PVA was 231 and 297, which is in line with the literature [34]. Degree of swelling is increased by adding the PVA. This is attributed to the increasing of hydrophilic groups (–OH) in the membrane preparation solution. Many research studies are confirmed that any system based on chitosan, in which blending with PVA increased the water uptake of the resulting material [35,36]. With increasing graphene content in the composite membranes, swelling degree increases. Increase in swelling might seem absurd as increase in PVA is due to hydrophilicity. Graphene is inherently hydrophobic; however, graphene is transparent to water to a certain degree. If a single sheet of graphene is placed on a hydrophilic substance, it behaves as a hydrophilic substance and increases the contact angle by only 1° to 2°, but this is possible only if the substance on which graphene is impregnated is hydrophilic due to long-range attraction force and not short ranged as in glass. [37] In this case, as graphene is not chemically bonded, it allows water to be contained and acts as a retainer/reservoir/pore for holding water and thus increasing membrane's porosity or hydrophilicity. The larger surface area of CHS/PVA/Gr is responsible for the increase in swelling degree compared to CHS/PVA and CHS [32].

3.3. Membrane porosity

In our study, CHS/PVA/Gr membrane is having a highest porosity (83 ± 2%) compare to CHS/PVA (71 ± 2%) and CHS (65 ± 2%) membrane. Highest porosity of membrane is because of the advance properties of the graphene.

3.4. FO performance evaluation of CHS/PVA/Gr membrane

In our study, baseline water flux value was 31.2 LMH. By use of 10 ppm algae solution, it reduced to 28.1 LMH. In one recent study, baseline water flux 24 LMH was reduced to 22.8, 21.6, and 19.2 for organic contains waste 10, 30, and 50 ppm, respectively [38]. Compare to baseline, the algae-containing water had a

Table 5
Conductivity, Porosity (%), and FO water flux for different membranes

Sr. No.	Name of membrane	Conductivity (× 10^{-6}) Sm	Porosity (%)	FO water flux (LMH)	Degree of swelling	Tensile strength (MPa)
1	CHS	2.77	65 ± 2	16.5	231	57.2 ± 1.6*
2	CHS/PVA	0.746	71 ± 2	21.8	297	71.6 ± 1.5*
3	CHS/PVA/Gr	24.51	83 ± 2	31.2	337	136 ± 1[a]

*CHS CHS/PVA, Degree of swelling and tensile strength (MPa) [32].

[a]CHS CHS/PVA Tensile strength (MPa) [31].

large drop in water flux. After eight hrs fouling experiment, the water flux was almost constant. This may be due to the switching of fouling mechanism from pore blocking to cake layer formation. All filtration experiments show that the permeate flux declined gradually at the initial stage, and after that showed a sudden drop midway through the fouling run. This may be due to the abrupt drop in water flux takes place when a cohesive cake is formed. Smaller parts of algae sticking to membrane provide surface area and act as a base for other algae to coagulate, thus increasing the algae concentration on the surface of the membrane rapidly and blocking effective membrane area for filtration. Therefore, permeate flux declined gradually at the initial stage, and after that showed a sudden drop midway through the fouling run [39]. Complete FO water flux pattern is clearly seen from Fig. 2. FO is known to have lower fouling propensity. Therefore, flux decline is usually slow and mild in many research studies. But, several recent studies on FO fouling have shown that substantial flux decline can occur due to inorganic scaling or synergistic effects between organic and inorganic foulants.

3.5. Organic fouling and cleaning experiments

3.5.1. Synthetic wastewater

Fouling experiment was carried out in petri dish/beaker with synthetic wastewater (Table 4). Before the experiments, macroscopic view of the new membrane was taken and represented in Fig. 3a CHS/PVA/Gr membrane filled and coated with graphene seemed much darker. From Fig. 3a, graphene can easily identified with black spots in the membrane. After fouling experiments, again macroscopic views are taken for fouled membranes (see Fig. 3b and 3c). After fouling, the membrane color was changed from blue to green because of organic matter deposition. From top view of Fig. 3c, it is clearly indentified the organic matters on the membranes are deposited by either layer or lump form. In cleaning process, electric field was

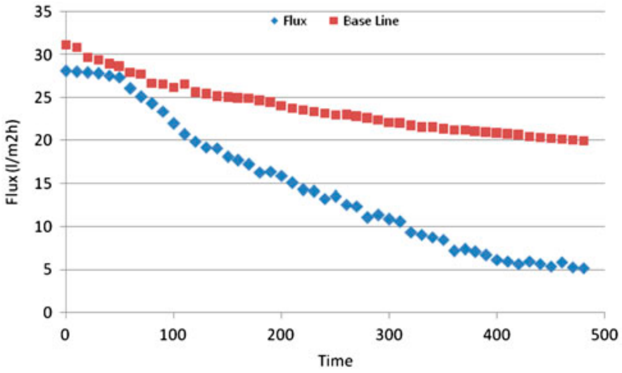

Fig. 2. Flux data with time for baseline and algae water.

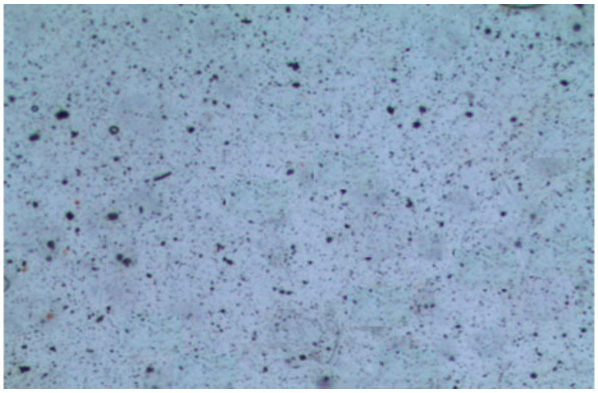

Fig. 3a. CHS/PVA/Gr membrane (before experiments and without fouling).

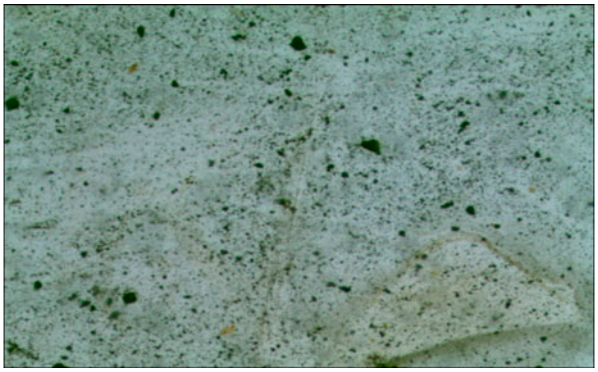

Fig. 3b. Foul CHS/PVA/Gr membrane (with graphene layer).

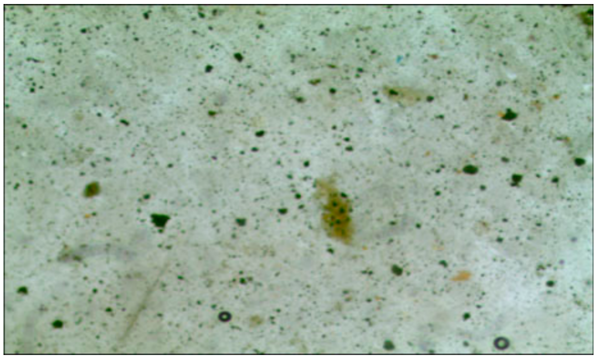

Fig. 3c. More foul CHS/PVA/Gr membrane (with graphene layer).

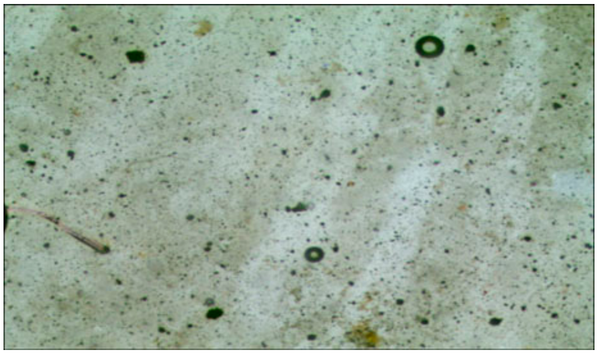

Fig. 3d. Vibration marks after electric cleaning for CHS/PVA/Gr membrane.

Fig. 4. Expected CHA/PVA/Gr membrane vibration.

used. As mention earlier that electric field generates vibration in graphene membrane based on graphene quantity and quality. Confirmation of the vibration is clearly seen on the membrane surface in the form of stretch marks or lines (see Fig. 3d). The expected graphene vibration is represented in Fig. 4.

3.5.2. *Algae-containing water*

In second set of experiments, as a draw solution 4 M NaCl solution was used. This higher concentration of draw solution will increase water flux in FO mode. This may be due to the generation of higher permeation drag force and pronounced concentration polarization of organic foulants (algae) near the membrane surface. In addition, the algae fouling layer that formed on the membrane surface could have hindered the back diffusive transport of salt, thereby accelerating the precipitation of salt on other side of membrane. Therefore, the reverse salt diffusion observed in this study was 0.015 gMH, which is very less compare to the literature values [5]. The large NaCl gradient induces reverse diffusion of NaCl from the draw solution side of the membrane to the feed side of the membrane. The salt that passed from the draw solution side of the membrane is trapped by the organic fouling layer leading to significant cake-enhanced osmotic pressure and resulted in low leakage of NaCl [40]. The mechanisms described above explain the dense fouling layer and the ensuing substantial flux decline during the fouling experiment when a higher initial water flux was employed [6]. After fouling, electric field was not applied, the water flux of CHS/PVA/Gr membrane in FO mode was very less. This is caused by the macroscopic lumpish of algae layer on membrane, blocking the space in pores, resulted in a much smaller pore size membrane. Then, after applying electric field to the membrane as seen in Fig. 5, the membrane washout may remove/wipe off some algae, resulting the flux for the fouled membrane increased and try to approach the level of initial water flux of membrane (Fig. 6) [39].

In general, membrane flux was increases when the electric field strength increases within certain range beyond this points, it is no longer economic. After reaching certain value (the critical potential), the flux remained almost constant [41]. At or above the critical potential can avoid the formation of filtration cake layer, but the high voltage means high-energy consumption/cost. To reduce energy consumption, an intermittent electric field only applied when the permeate flux has drastically declined which can also effectively suppress the membrane fouling [42]. In our study, two types of cleaning method are carried out.

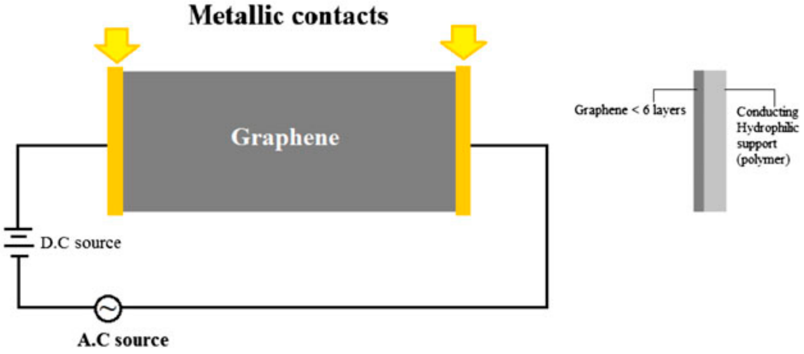

Fig. 5. Schematic of electric field applied to CHS/PVA/Gr membrane.

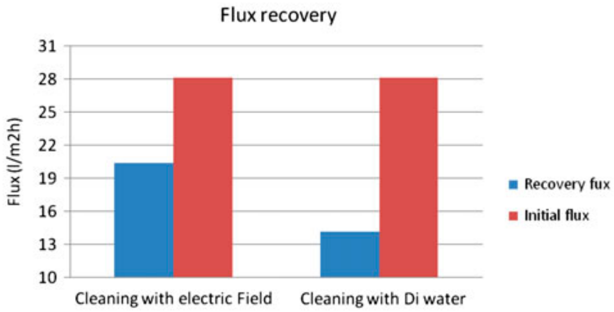

Fig. 6. Flux recovery graph.

The initial FO water flux value was 28.1 LMH. Therefore, intention of fouling method is to regain the initial flux after giving cleaning treatment. After cleaning experiments, the restore water flux values were 14.2 and 22.04 LMH for DI water and electric field cleaning method (Fig. 6), respectively.

Compare to DI water cleaning method an electric field method is more effective. DI water can remove only the ECP (external concentration polarization). But from the data, it can clear that electric field can remove ICP (internal concentration polarization) as well as ECP. Therefore, electric field can clean membrane efficiently by opening most of the pores compare to a widely used DI water method. Here, the % recovery of flux was 78% with electric field cleaning method. This may be due to nature of chitosan is biodegradable. Also, the sizes of single crystals of graphene were small, resulting less amplitude. The single crystal is costly so it was not used in this study. One more things that in this research study, instead of high conductive polymers (PANi, PPy, etc.), chitosan was used, which gives less conductivity to the prepared membrane. Therefore, in this study less vibration and resulting in less fouling efficiency is investigated. In further research, preparation of membrane becomes more effective and economical, if cheap large size few layered graphene will be used with highly conductive polymers. A similar concept is applied in preparing speakers out of graphene. Graphene's properties are not fully known and there is more to learn about it.

4. Conclusion

The CHS/PVA substrate membrane was modified by graphene nanosheet coating/filler on the porous side of the membrane. The modified membrane has high tensile strength, swelling ratio, porosity as well as high FO water flux. Fouling experiments (algae-containing wastewater) with the CHS/PVA/Gr membrane experienced less flux reduction. The CHS/PVA/Gr membrane achieved 78% recovery of flux by applying "electric field" cleaning method. Hence, graphene modified membrane showed effective improvement in fouling resistance of FO membranes. Since the direct coating of graphene as well as the cleaning process by "electric field" is simple, low cost and easy to operate without the requirement of high-energy input, it can be a potential method of scaled up for industrial *in situ* applications.

Acknowledgment

The second author (AAM) acknowledges the financial support for summer research fellowship from Sardar Vallabhbhai National Institute of Technology (SVNIT), Surat, India.

References

[1] A. Asatekin, A. Menniti, S.T. Kang, M. Elimelech, E. Morgenroth, A.M. Mayes, Antifouling nanofiltration membranes for membrane bioreactors from selfassembling graft copolymers, J. Membr. Sci. 285 (2006) 81–89.

[2] H. Shon, S. Vigneswaran, J. Cho, Comparison of physico-chemical pretreatment methods to seawater reverse osmosis: Detailed analyses of molecular weight distribution of organic matter in initial stage, J. Membr. Sci. 320 (2008) 151–158.

[3] X. Jin, X. Huang, E. Hoek, Role of specific ion interactions in seawater RO membrane fouling by alginic acid, Environ. Sci. Technol. 43 (2009) 3580–3587.

[4] J. Vrouwenvelder, J. van Paassen, J. van Agtmaal, M. van Loosdrecht, J. Kruithof, A critical flux to avoid biofouling of spiral wound nanofiltration and reverse osmosis membranes: Fact or fiction? J. Membr. Sci. 326 (2009) 36–44.

[5] Y. Zhou, S. Yu, C. Gao, X. Feng, Surface modification of thin film composite polyamide membranes by electrostatic self deposition of polycations for improved fouling resistance, Sep. Purif. Technol. 66 (2009) 287–294.

[6] C. Boo, M. Elimelech, S. Hong, Fouling control in a forward osmosis process integrating seawater desalination and wastewater reclamation, J. Membr. Sci. 444 (2013) 148–156.

[7] L. Liu, F. Zhao, J. Liu, F. Yang, Preparation of highly conductive cathodic membrane with graphene (oxide)/PPy and the membrane antifouling property in filtrating yeast suspensions in EMBR, J. Membr. Sci. 437 (2013) 99–107.

[8] M. Baoxia, M. Elimelech, Chemical and physical aspects of organic fouling of forward osmosis membranes, J. Membr. Sci. 320 (2008) 292–302.

[9] T. Huuhilo, P. Vaisanen, J. Nuortila-Jokinen, M. Nystrom, Influence of shear on flux in membrane filtration of integrated pulp and paper mill circulation water, Desalination 141 (2001) 245–258.

[10] O.A. Akoum, M.Y. Jaffrin, L. Ding, P. Paullier, C. Vanhoutte, An hydrodynamic investigation of microfiltration and ultrafiltration in a vibrating membrane module, J. Membr. Sci. 197 (2002) 37–52.

[11] O.A. Akoum, M.Y. Jaffrin, L.H. Ding, M. Frappart, Treatment of dairy process waters using a vibrating filtration system and NF and RO membranes, J. Membr. Sci. 235 (2004) 111–122.

[12] K. Takata, K. Yamamoto, R. Bian, Y. Watanabe, Removal of humic substances with vibratory shear enhanced processing membrane filtration, Desalination 117 (1998) 273–282.

[13] A.G. Boricha, Z.V.P. Murthy, Acrylonitrile butadiene styrene/chitosan blend membranes: Preparation, characterization and performance for the separation of heavy metals, J. Membr. Sci. 339 (2009) 239–249.

[14] J.C. Grunlan, A. Grigorian, C.B. Hamilton, A.R. Mehrabi, Effect of clay concentration on the oxygen permeability and optical properties of a modified poly(vinyl alcohol), J. Appl. Polym. Sci. 93 (2004) 1102–1109.

[15] A. Sang-Man, H. Jong-Wook, K. Jeong-Hoon, L. Yong-Taek, L. Soo-Bok, Pervaporation of fluoroethanol/water and methacrylic acid/water mixtures through PVA composite membranes, J. Membr. Sci. 247 (2005) 51–57.

[16] B. Van der Bruggen, Chemical modification of polyethersulfone nanofiltration membranes: A review, J Appl. Polym. Sci. 114 (1) (2009) 630–642.

[17] C.H. Yu, C.H. Wu, C.H. Lin, C.H. Hsiao, C.F. Lin, Hydrophobicity and molecular weight of humic substances on ultrafiltration fouling and resistance, Sep. Purif. Technol. 64 (2008) 206–212.

[18] H. Kim, A.A. Abdala, C.W. Macosko, Graphene/polymer nanocomposites, Macromolecules 43 (2010) 6515–6530.

[19] M.J. Allen, V.C. Tung, R.B. Kaner, Honeycomb carbon: A review of grapheme, Chem. Rev. 110 (2010) 132–145.

[20] S. Anandhavelu, S. Thambidurai, Single step synthesis of chitin/chitosan-based graphene oxide–ZnO hybrid composites for better electrical conductivity and optical properties, Electrochim. Acta. 90 (2013) 194–202.

[21] I. Tantis, G.C. Psarras, D. Tasis, Functionalized graphene–poly (vinyl alcohol) nanocomposites: Physical and dielectric properties, Polym. Lett. 6 (2012) 283–292.

[22] K. Iyakutti, V.J. Surya, K. Emelda, Y. Kawazoe, Simulation of ripples in single layer graphene sheets and study of their vibrational and elastic properties, Comput. Mater. Sci. 51 (2012) 96–102.

[23] C.G. Wang, L. Lan, Y.P. Liu, H.F. Tan, X.D. He, Vibration characteristics of wrinkled single-layered graphene sheets, Int. J. Solids Struct. 50 (2013) 1812–1823.

[24] J.P. Chen, C.Z. Yang, J.H. Zhou, X.Y. Wang, Study of the influence of the electric field on membrane flux of a new type of membrane bioreactor, Chem. Eng. J. 128 (2007) 177–180.

[25] A.B. Bourlinos, V. Georgakilas, R. Zboril, T.A. Steriotis, A.K. Stubos, C. Trapalis, Aqueous-phase exfoliation of graphite in the presence of polyvinylpyrrolidone for the production of water-soluble graphenes, Solid State Commun. 149 (2009) 2172–2176.

[26] W. Jing, Q. Changquan, Y.T. Chuyang, W. Rong, G.F. Anthony, Synthesis and characterization of flat-sheet thin film composite forward osmosis membranes, J. Membr. Sci. 372 (2011) 292–302.

[27] R.V. Linares, V. Yangali-Quintanilla, Z. Li, G. Amy, NOM and TEP fouling of a forward osmosis (FO) membrane: Foulant identification and cleaning, J. Membr. Sci. 421–422 (2012) 217–224.

[28] S. Vadukumpully, J. Paul, N. Mahanta, S. Valiyaveettil, Flexible conductive graphene/poly(vinyl chloride) composite thin films with high mechanical strength and thermal stability, Carbon 49 (2011) 198–205.

[29] Y. Xu, Y. Wang, J. Liang, Y. Huang, Y. Ma, X. Wan, Y. Chen, A hybrid material of graphene and poly (3,4-ethyldioxythiophene) with high conductivity, flexibility, and transparency, Nano Res. 2 (2009) 43–348.

[30] X.S. Du, M. Xiao, Y.Z. Meng, Facile synthesis of highly conductive polyaniline/graphite nanocomposites, Eur. Polym. J. 40 (2004) 1489–1493.

[31] L.F. Liu, J.D. Liu, B. Gao, F.L. Yang, Minute electric field reduced membrane fouling and improved performance of membrane bioreactor, Sep. Purif. Technol. 86 (2012) 106–112.

[32] M. Hazarika, T. Jana, Graphene nanosheets generated from sulfonated polystyrene/graphene nanocomposite, Compos. Sci. Technol. 87 (2013) 94–102.

[33] Y.S. Ye, M.Y. Cheng, X.L. Xie, J. Rick, Y.J. Huang, F.C. Chang, B.J. Hwang, Alkali doped polyvinyl alcohol/graphene electrolyte for direct methanol alkaline fuel cells, J. Power Sources 239 (2013) 424–432.

[34] S.B. Bahrami, S.S. Kordestani, H. Mirzadeh, P. Mansoori, Poly (vinyl alcohol)-chitosan blends: Preparation, mechanical and physical properties, Iran Polym. J. 12 (2003) 139–146.

[35] J.M. Yang, W.Y. Su, T.L. Leu, M.C. Yang, Evaluation of chitosan/PVA blended hydrogel membranes, J. Membr. Sci. 236 (2004) 39–51.

[36] R.K. Farag, R.R. Mohamed, Synthesis and characterization of carboxymethyl chitosan nanogels for swelling studies and antimicrobial activity, Molecules 18 (2013) 190–203.

[37] J. Rafiee, X. Mi, H. Gullapalli, A.V. Thomas, F. Yavari, Y. Shi, P.M. Ajayan, N.A. Koratkar, Wetting transparency of graphene, Nat. Mater. 11 (2012) 217–222.

[38] V. Parida, H.Y. Ng, Forward osmosis organic fouling: Effects of organic loading, calcium and membrane orientation, Desalination 312 (2013) 88–98.

[39] C. Boo, S. Lee, M. Elimelech, Z. Meng, S. Hong, Colloidal fouling in forward osmosis: Role of reverse salt diffusion, J. Membr. Sci. 390–391 (2012) 277–284.

[40] S. Lee, C. Boo, M. Elimelech, S. Hong, Comparison of fouling behavior in forward osmosis (FO) and reverse osmosis (RO), J. Membr. Sci. 365 (2010) 34–39.

[41] C. Chen, S. Rosenblatt, K.I. Bolotin, W. Kalb, P. Kim, I. Kymissis, H.L. Stormer, T.F. Heinz, J. Hone, Performance of monolayer graphene nanomechanical resonators with electrical readout, Nat. Nanotech. 4 (2009) 861–867.

[42] K. Akamatsu, W. Lu, T. Sugawara, S. Nakao, Development of a novel fouling suppression system in membrane bioreactors using an intermittent electric field, Water Res. 44 (2010) 825–830.

[43] S. Zhao, L. Zou, Effects of working temperature on separation performance, membrane scaling and cleaning in forward osmosis desalination, Desalination 278 (2011) 157–164.

[44] Y. Liu, M. Baoxia, Combined fouling of forward osmosis membranes: Synergistic foulant interaction

and direct observation of fouling layer formation, J. Membr. Sci. 407–408 (2012) 136–144.
[45] M.R. Abousnina, Oily wastewater treatment: Removal of dissolved organic components by forward osmosis, Master of Engineering — Research Thesis, School of Civil, Mining and Environmental Engineering, University of Wollongong, 2012.
[46] M. Baoxia, M. Elimelech, Silica scaling and scaling reversibility in forward osmosis, Desalination 312 (2013) 75–81.
[47] M.C. Porter, Handbook of industrial membrane. Noyes Publications, Park Ridge, NJ, 1990, pp. 136–259.
[48] S. Boonthanon, L.S. Hwan, S. Vigneswaran, Application of pulsating cleaning technique in crossflow microfiltration, Filt. Sep. 28 (1991) 199–201.
[49] J.J. Shen, R.F. Probstein, Turbulence promotion and hydrodynamic optimization in an ultrafiltration process, Ind. Eng. Chem. Process Des. Dev. 18 (1979) 547–554.
[50] H. Mallubhotla, G. Belfort, Flux enhancement during dean vortex microfiltration: 8. Further diagnostics, J. Membr. Sci. 125 (1997) 75–91.
[51] B.E. Reed, W. Lin, R. Viadero Jr., J. Young, Treatment of oily wastes using high-shear rotary ultrafiltration, J. Environ. Eng. ASCE 123 (1997) 1234–1242.
[52] C.M. Silva, D.W. Reeve, H. Husain, H.R. Rabie, K.A. Woodhouse, Model for flux prediction in high-shear microfiltration systems, J. Membr. Sci. 173 (2000) 87–98.
[53] C. Cabassud, S. Laborie, J.M. Lainé, How slug flow can enhance the ultrafiltration flux in organic hollow fibres, J. Membr. Sci. 128 (1997) 93–101.
[54] S. Chellam, J.G. Jacangelo, T.P. Bonacquisti, B.A. Schauer, Effect of pretreatment on surface water nanofiltration, J. Am. Water Works Assoc. 89 (1997) 77–89.
[55] A. Braghetta, J.G. Jacangelo, S. Chellam, M.L. Hotaling, B.A. Utne, DAF pretreatment: Its effect on MF performance, J. Am. Water Works Assoc. 89 (1997) 90–101.
[56] S.S. Adham, V.L. Snoeyink, M.M. Clark, J.-L. Bersillon, Predicting and verifying organics removal by PAC in an ultrafiltration system, J. Am. Water Works Assoc. 83 (1991) 81–91.
[57] M.R. Wiesner, S. Chellam, The promise of membrane technology, Environ. Sci. Technol. 33 (1999) 360A–366A.
[58] G. Belfort, R.H. Davis, A.L. Zydney, The behavior of suspensions and macromolecular solutions in crossflow microfiltration, J. Membr. Sci. 96 (1994) 1–58.
[59] P. Côté, H. Buisson, M. Praderie, Immersed membrane activated sludge process applied to the treatment of municipal wastewater, Water Sci. Technol. 38 (1998) 437–442.